Global Attitude Control via Contraction on Manifolds with Reference Trajectory and Optimization

Bee Vang[1] and Roberto Tron[2]

***Abstract*— In this paper, we present a simple geometric attitude controller that is globally, exponentially stable. To overcome the topological restriction, the controller is designed to follow a reference trajectory that in turn converges to the desired equilibrium (making it discontinuous in the initial conditions, but continuous in time). The system and reference dynamics are studied as a single augmented system that can be analyzed and tuned simultaneously. The controller's stability is proved using contraction analysis (on the manifold), and the bounds on the convergence rate can be found via a semi-definite program with linear matrix inequalities. Additionally, our approach allows the use of the Nelder-Mead algorithm to automatically select controller gains and reference trajectory parameters by optimizing the aforementioned bounds. The resulting controller is verified through simulations.**

I. INTRODUCTION

Rigid body attitude control is crucial to the successful operation of many systems; whether the task is to steer a vehicle, observe space with a satellite, or install a light bulb with a robotic arm. In particular, *drones* (multi-rotor aircrafts), typically rely on attitude control to maneuver [1]; quadrotors, for instance, have to first rotate its body in order to provide thrust in a specific desired direction.

Traditional controllers are generally developed using a specific parameterization of the space of rotations; however, these controllers often cannot guarantee global stability due to the additional singularities or ambiguities introduced by representations such as Euler angles and quaternions [2].

More recent approaches have instead worked directly on the underlying differential manifold (e.g., $SO(3)$ for rotations, $SE(3)$ for rotations and translations, $SO(3)\times\mathbb{S}^2$ for rotations with suspended load, etc.) of the configuration space. These geometric controllers [3]–[8], often combined with Lyapunov theory, have been shown to exhibit almost global stability with local exponential convergence (for $SO(3)$, the region is typically given by a ball of radius $\frac{\pi}{2}$ around the origin).

Hybrid approaches such as [9], [10], building on the work of [11], [12], represent the state of the art for attitude control. These hybrid controllers are able to achieve global stability by switching between multiple potential functions (inspired by non-hybrid controllers). The switching conditions are designed in a way as to avoid undesired equilibria or regions of slow convergence. However, these approaches are generally more complex and more computationally demanding than static feedback controllers. In addition, sudden changes in the control can lead to undesired system behaviors.

Another approach to achieve global stability is presented in [13], where the authors proposed a time-varying feedback controller that follows an intermediate reference trajectory converging to the desired equilibrium. The controller has the added benefit of being continuous in time (but discontinuous in the initial conditions), thereby bypassing the previously mentioned issue with hybrid controllers.

Most of the works cited above ensure stability by posing constraints on the tuning parameters. Such constraints generally derive from conditions on the eigenvalues of matrices, and may also depend on additional parameters from the analysis. As a result, the convergence conditions are difficult to decipher, and selecting good gains is challenging: the corresponding literature does not provide any method to identify suitable parameters, let alone ones that are optimal in some sense (e.g. providing the best convergence rate bounds).

In our previous work [14], we combined contraction analysis (as opposed to Lyapunov analysis) with optimization to study the stability of a system on the space of rotations. However, due to the topology and geometry of $SO(3)$, the proposed controller and framework can only achieve quasi-global exponential stability [15], [16].

Paper contributions. In this paper, we show that a simple, easy-to-implement geometric PD controller, can globally (as opposed to quasi-globally) and exponentially stabilize rigid body attitudes. To overcome the topological restriction on $SO(3)$, our controller introduces an intermediate time-varying reference as in [13] (even for stabilizing to a fixed equilibrium), but we allow for a more flexible choice of such trajectory. From an analytical standpoint, we avoid the introduction of time-varying systems by considering the reference as part of the state space, and we analyze and tune gains in this single augmented system using contraction theory and optimization. Although the analysis is, at a high level, similar to [14], we improve the framework by analyzing dynamics on product spaces (instead of a single bundle manifold), by proposing a less conservative and more general method to bound the contraction matrix eigenvalues, and by searching the gain space more efficiently.

II. PRELIMINARIES AND NOTATION

A. Riemannian Geometry

The work in this paper relies on core concepts from Riemannian geometry. A brief overview is provided; for a more in-depth discussion see, e.g., [17]. A rigid body's attitude in three dimensions can be uniquely represented by

This work was supported by the National Science Foundation grant NSF CMMI-1728277.

[1]Department of Mechanical Engineering, Boston University, Boston, MA 02215, USA {bvang@bu.edu}

[2]Department of Mechanical and System Engineering, Boston University, Boston, MA 02215, USA {tron@bu.edu}

a rotation matrix $R \in SO(3)$, where $SO(3) = \{R \in \mathbb{R}^{3\times 3} : R^T R = I_3, \det(R) = 1\}$. The *tangent space* at a point R on $SO(3)$ is denoted as $T_R SO(3) = \{RV : V \in \mathfrak{so}(3)\}$, where $\mathfrak{so}(3)$ is the set of all 3×3 skew-symmetric matrices. In addition, a tangent vector $W \in T_R SO(3)$ can be mapped to a vector $\omega \in \mathbb{R}^3$ using the hat $(\cdot)^\wedge$ and vee $(\cdot)^\vee$ operators:

$$\omega = \begin{bmatrix}\omega_1\\ \omega_2\\ \omega_3\end{bmatrix} \overset{(\cdot)^\wedge}{\underset{(\cdot)^\vee}{\rightleftarrows}} W = R\begin{bmatrix}0 & -w_3 & w_2\\ w_3 & 0 & -w_1\\ -w_2 & w_1 & 0\end{bmatrix}. \quad (1)$$

For convenience and clarity, we denote the hat operator at the identity $R = I_3$ as $\hat{\cdot}$ (i.e., without parentheses). Following this notation, the statements $W \in T_R SO(3)$: $W = (\omega)^\wedge = R\hat{\omega}$ represent the same tangent vector.

The *exponential* and *logarithm* maps defined at a rotation $R \in SO(3)$ locally transforms tangent vectors into points, and vice versa. The maps are denoted as $\exp_R : T_R SO(3) \to SO(3)$ and $\log_R : U_R \to T_R SO(3)$ where $U_R \subset SO(3)$ is the neighborhood around R for which $\exp_R$ is diffeomorphic. A metric $g : T_R SO(3) \times T_R SO(3) \to \mathbb{R}$ is a family of inner products defined on the tangent space. We use $g(\cdot,\cdot)_M$ to denote the metric defined by parameters contained in a matrix M (see §III for the precise definition). The covariant derivative $\nabla_X Y$ is a generalized derivative that takes in two smooth vector fields X, Y (e.g. $X, Y \in \mathfrak{X}(SO(3))$) and returns the variation of the field Y along the flow of X. In general the covariant derivative is not unique, however we use the unique torsion-free connection called the Levi-Civita connection derived from the metric g.

Second-order rigid body dynamics evolve on the tangent bundle $TSO(3) = \{(R, W) : R \in SO(3), W \in T_R SO(3)\}$, where the state variables are the rotations R and the angular velocities $\omega = W^\vee \in \mathbb{R}^3$ [17]. The *tangent space* at a point (R, W) is denoted as $T_W T_R SO(3) = \{(U, V) : U, V \in T_R SO(3)\}$, and since the tangent space of a tangent space can be identified with itself, we can represent tangent vectors in $T_W T_R SO(3)$ as vertically concatenated matrices using the stack function, e.g. $\mathrm{stack}(U, V) = \left[\begin{smallmatrix}U\\ V\end{smallmatrix}\right]$.

B. Rigid Body Dynamics

Rigid body rotations can be modeled using two reference frames: an inertial frame, and a body-fixed frame with origin at the center of mass. The equations of motion are

$$\begin{aligned}\dot{R} &= R\hat{\omega},\\ \dot{\omega} &= \Gamma - J^{-1}(\omega \times J\omega),\end{aligned} \quad (2)$$

where $R \in SO(3)$ is the rotation from the body to the inertial frame, $\omega \in \mathbb{R}^3$ is the angular velocity, $J \in \mathbb{R}^{3\times 3}$ is the inertia matrix, and $\Gamma \in \mathbb{R}^3$ is the total moment vector (control input), all expressed in the body frame.

C. Contraction Theory

In this section we review contraction theory [18], [19]. The motivation behind this theory is that if nearby trajectories of a system converge to some nominal motion, i.e., if the infinitesimal displacements δ_x between neighboring trajectories (vector fields, in differential geometry terminology) converge to zero, then the system is stable. Moreover, the convergence of the displacements can be shown by analyzing how the vector field generating the trajectories changes along the infinitesimal displacements. More formally, a nonlinear system $\dot{x} = f(x)$ on $\mathbb{R}^n$ (f viewed as a vector field) is contracting if, at any point $x \in \mathbb{R}^n$, the infinitesimal displacement between neighboring trajectories vanish exponentially fast,

$$g(\delta_x(t), \delta_x(t))_M = \|\delta_x(t)\|_M \le \|\delta_x(0)\|_M e^{-\beta t}. \quad (3)$$

The above observation leads to the following result.

Proposition 1 (Adapted from [18]): The system $\dot{x} = f(x)$ is contracting if there exist a positive definite constant matrix M such that

$$\frac{\mathrm{d}}{\mathrm{d}t}\left(\delta_x^T M \delta_x\right) = \delta_x^T\left(\frac{\partial f}{\partial x}^T M + M\frac{\partial f}{\partial x}\right)\delta_x \le -\beta \delta_x^T M \delta_x. \quad (4)$$

The general result considers matrices M that are functions of the state x and time t, although here we only consider constant matrices. The parameter β represents the minimum guaranteed exponential convergence rate of the system. Contraction analysis can be generalized to systems evolving on Riemannian manifolds.

Proposition 2 (Adapted from [19]): A system $\dot{x} = f(x)$ evolving on a manifold is contracting if there exist a metric g with Levi-Civita connection ∇ such that

$$g\left(\nabla_{\delta_x} f, \delta_x\right)_M \le -\beta g\left(\delta_x, \delta_x\right)_M \quad (5)$$

for any vector field δ_x.

Proposition 2 reduces to Proposition 1 when the manifold is Euclidean or the matrix M represents the coefficients of g after choosing local coordinates.

III. Attitude Controller

In this section, we present a geometric attitude controller for stabilizing a desired rotation $(R_d, \omega_d) \in TSO(3)$, and develop a framework to study closed-loop stability. Without loss of generality, we choose $R_d = I_3$ and $\omega_d = \mathrm{stack}(0, 0, 0)$.

Inspired by [13], we introduce a reference rotation R_{ref} that exponentially converges to the desired rotation R_d through a prescribed trajectory, and a geometric PD controller driving our rigid body dynamics R toward R_{ref}. We consider the dynamics of the rigid body, reference trajectory, and controller in a single system defined by a time-invariant vector field evolving on the product manifold $TSO(3) \times SO(3)$. The closed-loop vector field is discontinuous in the initial conditions, but continuous in time which is beneficial for practical applications, and we show that if the initial rotations (R, R_{ref}, R_d) are within some distance of each other, the system will converge to $R_d \in SO(3)$ exponentially fast.

More formally, the state of the augmented system is $(R, \omega, R_{ref}) \in TSO(3) \times SO(3)$ where $(R, \omega) \in TSO(3)$ and $R_{ref} \in SO(3)$; the tangent space at a point (R, ω, R_{ref}) is denoted as $T_{(\omega)^\wedge} T_R SO(3) \times T_{R_{ref}} SO(3)$. We also represent tangent vectors in this tangent space as vertically concatenated matrices, e.g. $\mathrm{stack}(X, Y, Z)$ for $(X, Y) \in T_{(\omega)^\wedge} T_R SO(3)$ and $Z \in T_{R_{ref}} SO(3)$.

Next, we choose two cost functions $\Psi_R(R, R_{ref})$ and $\Psi_{R_{ref}}(R_{ref}, R_d)$ which are bounded, star-convex (with Lipschitz continuous Hessian) [**?**] with respect to R_{ref} and R_d

in the neighborhood $U_{R_{ref}}$ and U_{R_d}, respectively, and such that they are zero when the arguments are identical. By specifying two cost functions, the behaviors of R and R_{ref} can be independently designed. Then, define the rotation and velocity errors as

$$e_R = \big(\mathrm{grad}_1(\Psi_R)\big)^\vee, \tag{6}$$

$$e_{R_{ref}} = \big(\mathrm{grad}_1(\Psi_{R_{ref}})\big)^\vee, \tag{7}$$

$$e_\omega = \omega - \omega_d = \omega, \tag{8}$$

where $\mathrm{grad}_i(\cdot)$ is the gradient operator with respect to the i-th argument. We then define a geometric PD controller of the form

$$\Gamma = J^{-1}\left(\omega \times J\omega\right) - k_d e_R - k_v e_\omega, \tag{9}$$

where the feedforward term cancels the gyroscopic effects, and k_d, k_v are positive feedback gains. In addition, let $-k_{ref}e_{R_{ref}}$ be the dynamics of the reference trajectory R_{ref} for some positive gain k_{ref}. The closed-loop equations for the augmented system become,

$$\begin{aligned} \dot{R} &= R\hat{\omega} \doteq f_R(R, \omega, R_{ref}), \\ \dot{\omega} &= -k_d e_R - k_v e_\omega \doteq f_\omega(R, \omega, R_{ref}), \\ \dot{R}_{ref} &= -k_{ref} R_{ref} \hat{e}_{R_{ref}} \doteq f_{R_{ref}}(R_{ref}) \end{aligned} \tag{10}$$

where the system dynamics evolve on the product manifold $TSO(3) \times SO(3)$. We denote this vector field as

$$\bar{\bar{Y}}_{sys}(R, \omega, R_{ref}) = (f_R, f_\omega, f_{R_{ref}}). \tag{11}$$

Remark 1: The dynamics for R_{ref} could be integrated into an explicit closed form; however the implicit form in (10) allows us to keep the system time-invariant.

We study the stability of (10) through four steps:

1) Derive the generalized contraction metric (5) for the closed-loop vector field $\bar{\bar{Y}}_{sys}$; this involves defining a metric on the product manifold and finding a corresponding covariant derivative;
2) Diagonalize and bound the contraction metric to obtain convex objectives and constraints; this includes bounding over rotations and velocities, and using Gershgorin discs;
3) Solve for the matrix M through optimization such that (5) is satisfied for given gains;
4) Automatically select the gains k_d, k_v, k_{ref} while maximizing β through a gradient-free bisection search.

1) Closed-Loop System and Contraction: The system $\bar{\bar{Y}}_{sys}(R, \omega, R_{ref})$ defines a vector field on the product manifold $TSO(3) \times SO(3)$. To begin, we choose a non-natural Riemannian metric of the form

$$\bar{\bar{g}}\left(\bar{\bar{X}}, \bar{\bar{Y}}\right)_M = \frac{1}{2}\,\mathrm{tr}\Big(\bar{\bar{X}}^T (M \otimes I_3)\bar{\bar{Y}}\Big) \tag{12}$$

where $\bar{\bar{X}}, \bar{\bar{Y}} \in T_{(\omega)^\wedge} T_R SO(3) \times T_{R_{ref}} SO(3)$,

$$M = \begin{bmatrix} m_1 & m_2 & m_6 \\ m_2 & m_3 & m_5 \\ m_6 & m_5 & m_4 \end{bmatrix} > 0, \tag{13}$$

and $\otimes$ is the Kronecker product. As a convention, all matrix inequalities in this paper denotes positive (semi-)definite matrices. This metric gives us six parameters $m_i \in \mathbb{R}, i \in 1, ..., 6$ to choose for satisfying the contraction condition (5). This, however, first requires finding a covariant derivative compatible with the general non-natural metric. On a product manifold, one can derive the covariant derivative corresponding to the *natural* metric from the covariant derivatives of the individual manifolds. A natural metric only pairs tangent vectors from the same manifolds and thus the covariant derivative is a linear combination of the individual manifold's derivatives (with the proper mapping). In our case, this corresponds to setting $m_5 = m_6 = 0$. However, in doing so, the set of possible metrics satisfying the contraction condition (5) is greatly reduced.

Instead, in this paper we show that it is possible to obtain the covariant derivative corresponding to the non-natural metric by using linear coordinate transformations to bring ourselves to the natural case.

Using Schur complement [21, Appx. A.5.5], we can find the linear transformation

$$J = \begin{bmatrix} 1 & 0 & 0 \\ 0 & 1 & 0 \\ m_6/m_4 & m_5/m_4 & 1 \end{bmatrix} \tag{14}$$

to reduce the metric to the natural case with parameters

$$M_n = \begin{bmatrix} m_1 - m_6^2/m_4 & m_2 - m_5 m_6/m_4 & 0 \\ m_2 - m_5 m_6/m_4 & m_3 - m_5^2/m_4 & 0 \\ 0 & 0 & m_4 \end{bmatrix} \tag{15}$$

with the matrix (13) transformed as $M = J^T M_n J$, and the non-natural metric (12) as

$$\bar{\bar{g}}(\bar{\bar{X}}, \bar{\bar{Y}})_M = \bar{\bar{g}}\Big((J \otimes I_3)\bar{\bar{X}}, (J \otimes I_3)\bar{\bar{Y}}\Big)_{M_n}. \tag{16}$$

Note that $M_n = \mathrm{blkdiag}(M_{n,TSO(3)}, M_{n,SO(3)})$, where

$$M_{n,TSO(3)} = \begin{bmatrix} m_1 - m_6^2/m_4 & m_2 - m_5 m_6/m_4 \\ m_2 - m_5 m_6/m_4 & m_3 - m_5^2/m_4 \end{bmatrix} \tag{17}$$

parametrizes a non-natural metric on $TSO(3)$ and

$$M_{n,SO(3)} = \begin{bmatrix} m_4 \end{bmatrix} \tag{18}$$

parametrizes a metric on $SO(3)$.

Remark 2: Transformed tangent vectors, e.g. $(J \otimes I_3)\bar{\bar{X}}$, must still be tangent vectors in $T_{(\omega)^\wedge} T_R SO(3) \times T_{R_{ref}} SO(3)$. Therefore, the individual components of the tangent vector must be transported to the correct tangent space. On $SO(3)$ there is a *natural* (or canonical) way given by the *left-translation*. For the transformation matrix (14), the two tangent vectors on $TSO(3)$ are scaled, left-translated from R to R_{ref}, and added to the tangent vector on $SO(3)$.

The product manifold of interest is $TSO(3) \times SO(3)$, and the covariant derivatives for $TSO(3)$ and $SO(3)$ are available [22], [23]. Let $\bar{\nabla}_{\bar{X}}\bar{Y}$ and $\nabla_X Y$ denote the covariant derivatives on $TSO(3)$ and $SO(3)$ compatible with the metrics given in (17) and (18), where $\bar{X}, \bar{Y} \in \mathfrak{X}(TSO(3))$ and $X, Y \in \mathfrak{X}(SO(3))$, respectively. Then the covariant derivative $\bar{\bar{\nabla}}_{\bar{\bar{X}}}\bar{\bar{Y}}$ on $TSO(3) \times SO(3)$ compatible with the metric (16) (equivalently (12)) is given as

$$\bar{\bar{\nabla}}_{\bar{\bar{X}}}\bar{\bar{Y}} = \mathrm{stack}(\bar{\nabla}_{\bar{X}}\bar{Y}, \nabla_X Y) \tag{19}$$

where $\bar{\bar{X}} = \mathrm{stack}(\bar{X}, X)$ and $\bar{\bar{Y}} = \mathrm{stack}(\bar{Y}, Y)$ are vector fields on the product manifold.

Remark 3: In computing the standard derivative component of the covariant derivative on $TSO(3)$ and $SO(3)$ for transformed vector fields, e.g. $\bar{\bar{\nabla}}_{(J\otimes I_3)\bar{\bar{X}}}(J \otimes I_3)\bar{\bar{Y}}$, the

derivative is taken along the original vector field $\bar{\bar{X}}$ because the curve is invariant under coordinate transformations.

The contraction condition for the closed-loop system can be computed by first finding the covariant derivative using (19) where the lower argument is an arbitrary vector $\delta_x = (J \otimes I_3)\text{stack}(R\hat{\zeta}, R\hat{\eta}, R_{ref}\hat{\nu})$ for $\zeta, \eta, \nu \in \mathbb{R}^3$ and the second argument is the transformed system dynamics vector field (10), i.e. $(J \otimes I_3)\bar{\bar{Y}}_{sys}$. Plugging the derivative and δ_x into the metric (16) and then into inequality (5), the contraction condition is

$$\begin{bmatrix}\zeta & \eta & \nu\end{bmatrix} \mathcal{M} \begin{bmatrix}\zeta & \eta & \nu\end{bmatrix}^T \leq 0 \tag{20}$$

where $\mathcal{M}$ is a symmetric matrix composed of six distinct block matrices given below:

$$\begin{aligned}\mathcal{M}_{1,1} &= -\frac{m_2 k_d}{2}\left(De_R + De_R^T\right) + \frac{1}{4}m_2'\hat{\omega}^2 \\ &\quad + m_1\beta I_3, \end{aligned}\tag{21}$$

$$\begin{aligned}\mathcal{M}_{2,1} &= -\frac{m_3 k_d}{2}De_R^T - \frac{k_d}{4}m_3'\hat{e}_R \\ &\quad + \frac{1}{8}m_3'\hat{\omega}^2 - \frac{1}{4}\left(m_2' - m_3' k_v\right)\hat{\omega} \\ &\quad + \frac{1}{2}\left(m_1 - m_2 k_v + 2m_2\beta\right) I_3, \end{aligned}\tag{22}$$

$$\mathcal{M}_{2,2} = \left(m_2 - m_3 k_v + m_3\beta\right) I_3, \tag{23}$$

$$\begin{aligned}\mathcal{M}_{3,1} &= \frac{k_d}{2}\left(m_2 - m_5\right) De_R^T + \frac{m_5 m_6 k_d}{4m_4}\hat{e}_R \\ &\quad - \frac{m_6 k_{ref}}{2}De_{R_{ref}} + \frac{m_6 k_{ref}}{4}\hat{e}_{R_{ref}} \\ &\quad + \frac{m_6^2 - m_5 m_6 k_v}{4m_4}\hat{\omega} + m_6\beta I_3, \end{aligned}\tag{24}$$

$$\begin{aligned}\mathcal{M}_{3,2} &= \frac{m_3 k_d}{2}De_R^T + \frac{m_5^2 k_d}{4m_4}\hat{e}_R - \frac{m_5 k_{ref}}{2}De_{R_{ref}} \\ &\quad + \frac{m_5 k_{ref}}{4}\hat{e}_{R_{ref}} + \frac{m_5 m_6 - m_5^2 k_v}{4m_4}\hat{\omega} \\ &\quad + \frac{1}{2}\left(m_6 - m_5 k_v + 2m_5\beta\right) I_3, \end{aligned}\tag{25}$$

$$\begin{aligned}\mathcal{M}_{3,3} &= \frac{m_5 k_d}{2}\left(De_R + De_R^T\right) + m_4\beta I_3 \\ &\quad - \frac{m_4 k_{ref}}{2}\left(De_{R_{ref}} + De_{R_{ref}}^T\right), \end{aligned}\tag{26}$$

where

$$m_2' = m_2 - \frac{m_5 m_6}{m_4}, \quad m_3' = m_3 - \frac{m_5^2}{m_4} \tag{27}$$

and De_R and $De_{R_{ref}}$ are the differentials of the rotation errors (6) and (7) at R and R_{ref}, respectively.

Remark 4: To simplify notation and for the particular cost functions of interest (42), the Hessian of Ψ_R ($\Psi_{R_{ref}}$) taken at R_{ref} (I_3) is given by the matrix transpose De_R^T ($De_{R_{ref}}^T$, respectively). The analysis is identical for the general case.

2) Contraction Matrix Bounds: Notice that the requirement (20) is equivalent to $\mathcal{M} \leq 0$, which is satisfied if the maximum eigenvalue of $\mathcal{M}$ is nonpositive. In addition, (20) has to be considered for all possible (R, ω, R_{ref}), resulting in an infinite number of constraints. Furthermore, although the analytical equations for all eigenvalues of $\mathcal{M}$ are non-convex with respect to $m_i, i = 1, ..., 6$, the *elements* of $\mathcal{M}$ are at most quadratic in the same variables (with m_4 fixed).

Our next step is to derive convex constraints for bounding the eigenvalues of $\mathcal{M}$ using the following strategy:

1) Perform a similarity transformation such that the block-diagonal matrices of $\mathcal{M}$ are mostly diagonalized and depend on the eigenvalues of De_R and $De_{R_{ref}}$;
2) Bound the eigenvalues using Gershgorin discs, and extract quadratic constraints that depend on the singular values of each off-diagonal block matrix;
3) Convexify all non-convex quadratic constraints.

In the first step, we choose a transformation matrix

$$S = \begin{bmatrix} P & 0_3 & 0_3 \\ 0_3 & Q & 0_3 \\ 0_3 & 0_3 & Q \end{bmatrix}, \tag{28}$$

where P, Q are orthogonal matrices, i.e. $P^T P = Q^{\mathrm{T}} Q = I_3$, that diagonalize $\left(De_R + De_R^T\right)$ and $\left(De_{R_{ref}} + De_{R_{ref}}^T\right)$, respectively [24, Thm. 4.1.5]. Then the matrix $\mathcal{M}$ can be transformed, via $S^T\mathcal{M}S$, such that the block-diagonal matrices are mostly diagonalized,

$$\begin{aligned}\left[S^T\mathcal{M}S\right]_{1,1} &= -m_2 k_d \text{Re}(\Lambda_R) + \frac{1}{4}P^T m_2'\hat{\omega}^2 P \\ &\quad + m_1\beta I_3 \end{aligned}\tag{29}$$

$$\left[S^T\mathcal{M}S\right]_{2,1} = Q^T\mathcal{M}_{2,1}P, \quad \left[S^T\mathcal{M}S\right]_{2,2} = \mathcal{M}_{2,2} \tag{30}$$

$$\left[S^T\mathcal{M}S\right]_{3,1} = Q^T\mathcal{M}_{3,1}P, \quad \left[S^T\mathcal{M}S\right]_{3,2} = Q^T\mathcal{M}_{3,2}Q \tag{31}$$

$$\begin{aligned}\left[S^T\mathcal{M}S\right]_{3,3} &= -m_4 k_{ref}\text{Re}(\Lambda_{R_{ref}}) + m_4\beta I_3 \\ &\quad + \frac{m_5 k_d}{2}Q^T\left(De_R + De_R^T\right)Q \end{aligned}\tag{32}$$

where $\text{Re}(\cdot)$ is the real part of a complex matrix, Λ_R and $\Lambda_{R_{ref}}$ are the diagonal matrix containing the eigenvalues of De_R and $De_{R_{ref}}$, respectively.

Next since similar matrices have the same eigenvalues, we focus on bounding the eigenvalues of $S^T\mathcal{M}S$. A general result to bound the eigenvalues of any square matrix is given by the Gershgorin discs theorem (see [24]). We show that the Gershgorin disc bounds on $S^T\mathcal{M}S$ lead to eigenvalue bounds that do not depend directly on the states (R, ω, R_{ref}), but geometric parameters and/or eigenvalues in $\Lambda_R, \Lambda_{R_{ref}}$. To do so, we introduce a useful lemma.

Lemma 1: For any $n \times n$ matrices A and B, the maximum absolute row sum, $\|A + B\|_\infty$, is bounded by the sum of their maximum singular values $\sigma_{\max}$,

$$\max_{1\leq i\leq n}\sum_{j=1}^{n}|a_{i,j} + b_{i,j}| \leq \sqrt{n}\big(\sigma_{\max}(A) + \sigma_{\max}(B)\big) \tag{33}$$

Proof: By norm equivalence, $\|A+B\|_\infty \leq \sqrt{n}\|A+B\|_2$. Then by Cauchy-Schwarz, $\|A+B\|_2 \leq \|A\|_2 + \|B\|_2$. Finally, $\|\cdot\|_2 = \sigma_{\max}(\cdot)$ and the proof is complete [24, Chap. 5.6]. ■

Applying Gershgorin, the centroid of the discs are given by the diagonal elements of $\left[S^T\mathcal{M}S\right]_{i,i}$. However for the case where $i = 1$ and 3, there are diagonal elements with dependencies on P or Q, e.g. $\frac{1}{4}P^T m_2'\hat{\omega}^2 P$. It is difficult to extract a closed-form expression for the diagonal elements of these matrices since P and Q are general orthogonal matrices, and the matrix being multiplied also depends on the states (R, ω, R_{ref}). This issue can be resolved by considering

these diagonal elements and their corresponding block matrix as part of the disc's radius.

The radii are then computed by taking the absolute row sum of all off-diagonal elements. Again there are difficulties in extracting closed-form expressions for these terms due to P, Q, and the dependencies on (R, ω, R_{ref}). Nonetheless, since we seek bounds that encompass all states, we consider the worst case (or largest radius components). In other words, for each off-diagonal block matrix, $\left[S^T\mathcal{M}S\right]_{i,j}, i \neq j$, the absolute row sum of any row is bounded by the maximum absolute row sum, $\|\left[S^T\mathcal{M}S\right]_{i,j}\|_\infty, i \neq j$. Furthermore, the dependencies on P and Q can be removed since they are orthogonal; therefore any *induced* matrix norm of products involving them are invariant, i.e. $\|\left[S^T\mathcal{M}S\right]_{i,j}\|_\infty = \|\mathcal{M}_{i,j}\|_\infty$ [24, Chap. 5.6]. Thus, Lemma 1 can be used to compute the radii of the Gershgorin discs.

Also, since the radius of each block row is bounded by the same value, and $\mathrm{Re}(\Lambda_R)$ and $\mathrm{Re}(\Lambda_{R_{ref}})$ are strictly positive and bounded, the centroid producing the largest bound is given by the smallest real eigenvalue.

The maximum bounds on the eigenvalues of $S^T\mathcal{M}S$, using the relaxations above on (29)-(**??**), results in:

$$\mathcal{D}_1 = -m_2 k_d \min\Big(\mathrm{dg}\big(\mathrm{Re}(\Lambda_R)\big)\Big) + \mathcal{B}_{2,1} + \mathcal{B}_{3,1} + \sqrt{3}\max\left|\frac{1}{4}m_2'\|\omega\|^2\begin{bmatrix}0\\-1\end{bmatrix} + m_1\beta\right|, \tag{34}$$

$$\mathcal{D}_2 = m_2 - m_3 k_v + m_3\beta + \mathcal{B}_{2,1} + \mathcal{B}_{3,2}, \tag{35}$$

$$\mathcal{D}_3 = -m_4 k_{ref}\min\Big(\mathrm{dg}\big(\mathrm{Re}(\Lambda_{R_{ref}})\big)\Big) + \mathcal{B}_{3,1} + \mathcal{B}_{3,2} + \sqrt{3}\max\left|m_5 k_d \mathrm{dg}\big(\mathrm{Re}(\Lambda_R)\big) + m_4\beta I_3\right|, \tag{36}$$

where

$$\mathcal{B}_{2,1} = \sqrt{3}\left|-\frac{1}{8}m_3'\|\omega\|^2\right| + \sqrt{3}\left|-\frac{1}{4}\left(m_2' - m_3' k_v\right)\|\omega\|\right| + \sqrt{3}\max\left|\frac{(m_1 - m_2 k_v + 2\beta m_2) - m_3 k_d \mathrm{dg}(\Lambda_R)}{2}\right| + \sqrt{3}\left|\frac{k_d}{4}m_3'\theta_R\right|, \tag{37}$$

$$\mathcal{B}_{3,1} = \sqrt{3}\max\left|\frac{k_d}{2}\left(m_2 - m_5\right)\mathrm{dg}(\Lambda_R)\right| + \sqrt{3}\left|\frac{m_5 m_6 k_d}{4m_4}\theta_R\right| + \sqrt{3}\left|\frac{m_6^2 - m_5 m_6 k_v}{4m_4}\|\omega\|\right| + \sqrt{3}\left|\frac{m_6 k_{ref}}{4}\theta_{R_{ref}}\right| + \sqrt{3}\max\left|-\frac{m_6 k_{ref}}{2}\mathrm{dg}\big(\Lambda_{R_{ref}}\big) + m_6\beta\right|, \tag{38}$$

$$\mathcal{B}_{3,2} = \sqrt{3}\max\left|\frac{m_3 k_d}{2}\mathrm{dg}\big(\Lambda_R\big) + \frac{1}{2}\left(m_6 - m_5 k_v\right)\right| + \max\left|-\frac{m_5 k_{ref}}{2}\mathrm{dg}\big(\Lambda_{R_{ref}}\big) + m_5\beta\right| + \sqrt{3}\left|\frac{m_5^2 k_d}{4m_4}\theta_R\right| + \sqrt{3}\left|\frac{m_5 m_6 - m_5^2 k_v}{4m_4}\|\omega\|\right| + \sqrt{3}\left|\frac{m_5 k_{ref}}{4}\theta_{R_{ref}}\right|, \tag{39}$$

and $\|\omega\|$, θ_R, and $\theta_{R_{ref}}$ are the norms of ω, e_R, and $e_{R_{ref}}$ respectively, and $\mathrm{dg}(\cdot)$ extracts the diagonal elements of a matrix as a vector or the inverse for a vector argument. The eigenvalue bounds are still state dependent (through Λ_R, $\Lambda_{R_{ref}}$, θ_R, $\theta_{R_{ref}}$, $\|\omega\|$). However, these can be reduced to a finite number of bounds using the following remarks. As a result, the constraints on $S^T\mathcal{M}S$ (and $\mathcal{M}$) will only depend on $m_i, i = 1, ..., 6$.

Remark 5: The θ_R and $\theta_{R_{ref}}$ parameters represent a distance error between any two rotations on $SO(3)$ and are state dependent. To remove the state dependency, since (37)-(39) are linear with respect to θ_R and $\theta_{R_{ref}}$, we can select maximum values $\theta_{R,\max}$ and $\theta_{R_{ref},\max}$ that geometrically specify a region of the manifold (further below, we show that this region only limits the initial conditions of R_{ref}), without affecting the overall convergence. Additionally, the eigenvalues Λ_R and $\Lambda_{R_{ref}}$ are also bounded [**?**] therefore appropriate values can be selected to maximize the bounds (34)-(36) in the region of $\theta_{R,\max}$ and $\theta_{R_{ref,\max}}$.

Remark 6: The eigenvalue bounds scale with $\|\omega\|$. There might not exist a set of $m_i, i = 1, ..., 6$ that satisfies $\mathcal{M} \leq 0$ for all $\|\omega\|$, since $\omega \in \mathbb{R}^3$ is unbounded. Therefore, we assume that there is a bound on the initial speed $\|\omega\|_{\max}$, as is standard in the literature [5], [6].

Remark 7: In computing $\mathcal{B}_{2,1}, \mathcal{B}_{3,1}, \mathcal{B}_{3,2}$, we assumed that De_R and De_R^T ($De_{R_{ref}}$ and $De_{R_{ref}}^T$, respectively) share the same eigenvectors and thus the singular value is simply $\max(|\Lambda_R|)$ ($\max(|\Lambda_{R_{ref}}|)$, respectively). This is the case for our particular cost function (42), but the process and form of the bounds are similar for the general case.

The last step is to produce convex constraints from the bounds (34)-(36). First, observe that each bound can be expanded into γ_i bounds where the $\max$ function is replaced by one of its γ_i arguments, considering all possible combinations if multiple $\max$ are present. Similarly, α_k absolute values can be expanded into 2^{α_k} bounds by replacing them with the combinations of positive and negative arguments. For example, (34) has $\gamma_1\gamma_2\gamma_3\gamma_4 = 2 \cdot 3 \cdot 3 \cdot 3 = 54$ bounds after expanding its four $\max$ functions, which result in $54 \cdot 2^{10}$ bounds after expanding the 10 absolute value terms.

Remark 8: Although there are many constraints, they only need to be solved offline during the *design* phase. In implementation, the controller is a simple static feedback. The number of constraints is easily handled by modern solvers. In the case of the CVX modeling environment, the constraints can be entered without the $\max$ and absolute value function expansions if written with only linear variables. In practice, the total number of constraints can be drastically reduced depending on the cost functions $\Psi_R, \Psi_{R_{ref}}$. In some cases, individual terms can be combined or written without absolute values which reduces the number of constraints exponentially.

Expanding each bound (34)-(36) and by inspection, the resulting bounds can be written in quadratic matrix form since they are at most quadratic with respect to $m_i, i = 1, ..., 6$ and m_4 fixed (see Remark 11 below). In addition, the bounds are constrained to be less than or equal to zero to satisfy (20). Define $y = \mathrm{stack}(m_1, m_2, m_3, m_5, m_6)$, then each of the constraints can written as

$$y^T A_j y + B_j^T y + C_j(m_4) \leq 0,\ j = 1, ..., \sum_1^3 2^{\alpha_k}\Pi\gamma_i, \tag{40}$$

where $A_j^T = A_j$, $B_j \in \mathbb{R}^5$, and $C_j \in \mathbb{R}$. The A_j's are sparse with only non-zero elements in the bottom right 2×2 block matrix and are, in general, non-convex ($A_j \not\succeq 0$).

Remark 9: Since A_j is real and symmetric, it can be diagonalized by some orthogonal matrix V, i.e. $A_j = V\Lambda V^T$ where Λ is the diagonal eigenvalues matrix. Next, choose $A_j' = V\Lambda' V^T$ where $\Lambda'_{i,i} = \max(0, -\Lambda_{i,i})$ and zero elsewhere. Then, the constraint involving A_j can be made convex if it is replaced with $A_j + A_j' \geq 0$. By making (40) convex, the constraints can be solved quickly using standard convex solvers.

3) Feasibility Problem: In this section, we formulate a feasibility problem to bound the maximum eigenvalue of the contraction matrix (20) using convex constraints from (40) to solve for (13) under the assumption that all other parameters are given. The feasibility problem can be solved as a semidefinite program (SDP).

Theorem 1: The closed-loop system given in (10) with controller (9) is globally, exponentially stable with minimum convergence rate $\beta > 0$ for all $R \in SO(3)$, if there exist $m_i, i = 1, ..., 6$ satisfying,

$$\begin{bmatrix} -B_j^T y - C_j & y^T \left(A_j + A_j'\right)^{1/2} \\ \left(A_j + A_j'\right)^{1/2} y & I_5 \end{bmatrix} \geq 0$$

$$j = 1, ..., \sum_1^3 (2^{\alpha_k})\Pi\gamma_i, \quad \Big(\text{eigenvalue bounds}\Big)$$

$$\begin{bmatrix} m_1 & m_2 & m_6 \\ m_2 & m_3 & m_5 \\ m_6 & m_5 & m_4 \end{bmatrix} > 0, \quad \Big(\text{metric on } TSO(3) \times SO(3)\Big) \tag{41}$$

for given k_d, k_v, k_{ref}, β, $\|\omega\|_{\max}$, $\theta_{R,\max}$, $\theta_{R_{ref},\max}$, m_4, $\theta_{R,\max} + \theta_{R_{ref},\max} \geq \pi$, and $y = \text{stack}(m_1, m_2, m_3, m_5, m_6)$.

Proof: The constraints in (40) bounds the maximum possible eigenvalue of $\mathcal{M}$ for all states (R, ω, R_{ref}) within the regions specified by the parameters $\theta_{R,\max}, \|\omega\|_{\max}, \theta_{R_{ref},\max}$. The convex constraints, using Remark 9, can be transformed into equivalent linear matrix inequalities (LMI) via the Schur complement lemma [21, Appx. A.5.5] resulting in the first set of constraints. The second set of constraints is the requirement stemming from the non-natural metric (12) on the product manifold. Then, if suitable $m_i, i = 1, ..., 6$ are found, the system is converging exponentially by contraction theory since (20) is always nonpositive.

Furthermore, the set of states R that are exponentially converging is given by $\Phi_R = \{R \in SO(3) : \theta_R(R, I_3) \leq \theta_{R,\max} + \theta_{R_{ref},\max}\}$. To see this, note that R is converging if there exist a R_{ref} such that $\theta_R(R, R_{ref}) \leq \theta_{R,\max}$. Similarly, the set of converging R_{ref} is given by $\Phi_{R_{ref}} = \{R_{ref} \in SO(3) : \theta_{R_{ref}}(R_{ref}, I_3) \leq \theta_{R_{ref},\max}\}$. Then, the set Φ_R must include $\Phi_{R_{ref}}$ and all rotations up to $\theta_{R,\max}$ distance away. Since $\theta_{R,\max} + \theta_{R_{ref},\max} \geq \pi$, Φ_R completely covers $SO(3)$.

Finally, the closed-loop vector field (11) is the gradient of the Lyapunov function $V(R, \omega, R_{ref}) = \|\bar{Y}_{sys}\|_M^2$ where the norm is with respect to the metric (12), and thus the contraction region is forward-invariant and forward complete by [18, Corollary 5.1]. Since Φ_R covers $SO(3)$, the system is globally, exponentially stable. ■

Remark 10: Due to the relaxations used to find $m_i, i = 1, ..., 6$, the parameters $\theta_{R,\max}, \|\omega\|_{\max}, \theta_{R_{ref},\max}$ represent a conservative contraction region of the state space. It is possible to back-solve (e.g. numerically) for the actual limiting parameters (states). However our analysis guarantees exponential convergence if the system starts in the contracting region $R_0 \in \Phi_R$, $\|\omega\|_0 \leq \|\omega\|_{\max}$ and $R_{ref,0} \in \Phi_{R_{ref}} \cap \theta_R(R_0, R_{ref,0}) \leq \theta_{R,\max}$, which is sufficient.

Remark 11: The contraction metric (20) is homogeneous in M. If a particular solution M^* exist, then any scaling of M^* is also a solution. Therefore, we add the constraint $m_4 = 1$ to improve the numerical stability and to remove some nonlinearity in the eigenvalue bounds (34)-(36).

4) Automated Gain Selection: The problem in Theorem 1 might be infeasible for the given parameters, and even if it is feasible, it might not provide the best convergence guarantees. In this section, we introduce Algorithm 1, a gradient-free bisection search algorithm that uses the Nelder-Mead algorithm [25] to automatically select the best gains k_d^*, k_v^*, k_{ref}^* with the largest minimum convergence rate β^* for given parameters $\|\omega\|_{\max}, \theta_{R,\max}$ and $\theta_{R_{ref},\max}$. The Nelder-Mead algorithm is used because it can search quickly around desired gains for a local optimal and it can optimize over any general nonlinear scalar-valued function (as the one generated by the bisection search here).

Algorithm 1 Gradient-free bisection search algorithm to find k_d^*, k_v^*, k_{ref}^* with largest minimum convergence rate β^* satisfying Theorem 1. The system input parameters are the maximum angular speed $\|\omega\|_{\max}$, distance errors $\theta_{R,\max}, \theta_{R_{ref},\max}$, and initial desired gains $gainsList$.

Require: $gainsList, \|\omega\|_{\max}, \theta_{R,\max}, \theta_{R_{ref},\max}$
  for $[k_d, k_v, k_{ref}]$ in $gainsList$ **do**
    $[k_d', k_v', k_{ref}', \beta'] \leftarrow$ NelderMead(k_d, k_v, k_{ref}) {
      $\beta' \leftarrow$ bisectionSearch(k_d', k_v', k_{ref}') {
        Solve feasibility problem (41)}}
    $optParams \leftarrow [k_d', k_v', k_{ref}', \beta']$
  end for
  return $[k_d^*, k_v^*, k_{ref}^*, \beta^*] =$ maxConRate$(optParams)$

The underlying principle of the algorithm is that it solves the feasibility problem (41) multiple times with different gains (generated by Nelder-Mead) and convergence rates (generated by bisection search), ultimately selecting the combination with the largest guaranteed minimum convergence rate β.

Remark 12: The general strategy presented in Algorithm 1 can be used to select gains for any controller with explicit bounds on the convergence rate (such as the one from [6]). In our case, with results based on contraction and convex optimization, the implementation is greatly simplified.

Remark 13: If the $gainsList$ is densely defined and the number of test iterations in the Nelder-Mead algorithm is one, then Algorithm 1 reduces to a brute force grid-search.

However, a more sparse $gainsList$ utilizing the Nelder-Mead algorithm can sample the gain space more efficiently.

IV. Results and Simulation

In this section, we validate the controller and theory presented in Section III with a simulation. Recall that we are stabilizing to the point $R_d = I_3$ and $\omega_d = \text{stack}(0,0,0)$. To begin, we choose Ψ_R and $\Psi_{R_{ref}}$ to be (with $r \in \{R, R_{ref}\}$),

$$\Psi_r(R_1, R_2) = \frac{1}{2} d(R_1, R_2)^2 = \frac{1}{2} \| \left(\log_{R_1} R_2 \right)^\vee \|^2, \quad (42)$$

which is the squared geodesic distance on $SO(3)$ with metric [26]

$$g\left(R\hat{\alpha}, R\hat{\xi}\right) = \frac{1}{2} \text{tr}\left(\hat{\alpha}^T \hat{\xi}\right). \quad (43)$$

Then, the gradient of Ψ_r is given by [27, Prop. 2.2.1] as

$$\text{grad}_1(\Psi_r) = -\log_{R_1} R_2 = R_1 R_2^T \log_{R_2} R_1. \quad (44)$$

Remark 14: Note that our formulation separates the metric used to compute the errors and control (43) from the metric for proving convergence (16).

Since $\hat{e}_r$ and its differential De_r share the same eigenvectors [27], they can be simultaneously diagonalized resulting in diagonal eigenvalue matrices $\Lambda_{\hat{e}_r} = \text{dg}\left(\text{stack}(0, \theta_r i, -\theta_r i)\right)$ and $\Lambda_r = \text{dg}\left(\text{stack}(1, \frac{\theta_r}{2}\cot\frac{\theta_r}{2} + \frac{\theta_r}{2} i, \frac{\theta_r}{2}\cot\frac{\theta_r}{2} - \frac{\theta_r}{2} i)\right)$ [27, Prop. E.2.1] where $\cot(\cdot)$ is the cotangent function, i is the imaginary unit, and $\theta_r = \| \left(\log_{R_1} R_2 \right)^\vee \|$. The θ_r parameter represents the geodesic distance between any two rotations on $SO(3)$ with respect to the metric (43), and is bounded between 0 and π [27]. Thus, the real part of the eigenvalue $\frac{\theta_r}{2}\cot\frac{\theta_r}{2} \in (0,1)$ is continuous for $\theta_r \in [\pi, 0]$ and $\min\left(\text{dg}\left(\text{Re}(\Lambda_r)\right)\right) = \frac{\theta_r}{2}\cot\frac{\theta_r}{2}$.

Next, with Remark 8 in mind, some terms in the off-diagonal block matrices of $\mathcal{M}$ can be combined when computing the singular values. For example, from (22) these two terms can be combined,

$$\sigma_{\max}\left(-\frac{m_3 k_d}{2} De_R^T - \frac{m_3 k_d}{4}\hat{e}_R\right) = \frac{m_3 k_d}{2} \quad (45)$$

because De_R^T and $\hat{e}_R$ share the same eigenvectors, $m_3, k_d, \text{Re}(\Lambda_R) > 0$, and $\max\left(\text{dg}(\text{Re}(\Lambda_R))\right) = 1$. After expanding the bounds (34)-(36), our cost function resulted in 3072 constraints which is considerably less than expected.

The system and Algorithm 1 parameters are reproduced in Table I; the initial attitude R_0 has been selected to be the maximum distance (π) away from the identity I_3, the initial reference rotation $R_{ref,0}$ has been randomly selected to be $\theta_{R_{ref},\max}$ distance away from the identity and $\theta_{R,\max}$ from R_0, and the initial angular velocity $\omega_0 = \frac{\left(\log_{R_0} R_{ref,0}\right)^\vee}{\| \left(\log_{R_0} R_{ref,0}\right)^\vee \|}$. The initial gains k_d, k_v are selected near the optimal results in [14] with varying k_{ref}. The algorithm results are shown in Table II with

$$M = \begin{bmatrix} 0.0347 & 0.0003 & 0.0140 \\ 0.0003 & 0.0001 & 0.0003 \\ 0.0140 & 0.0003 & 1.000 \end{bmatrix} \quad (46)$$

where we solved the feasibility problem in Theorem 1, utilizing Remark 11 to constrain $m_4 = 1.000$, using the CVX modeling system [28] and SDPT3 solver [29]. The algorithm found a metric guaranteeing minimum convergence rate $\beta = 0.4022$, although the actual rate is in fact faster (see Fig. 1). The looseness of the bound could be due to several reasons, such as the use of the Gershgorin discs, the singular value relaxation, convex constraints relaxation, and the fact that the bound needs to hold in a large convergence basin ($\theta_{R,\max} + \theta_{R_{ref},\max} = \pi$).

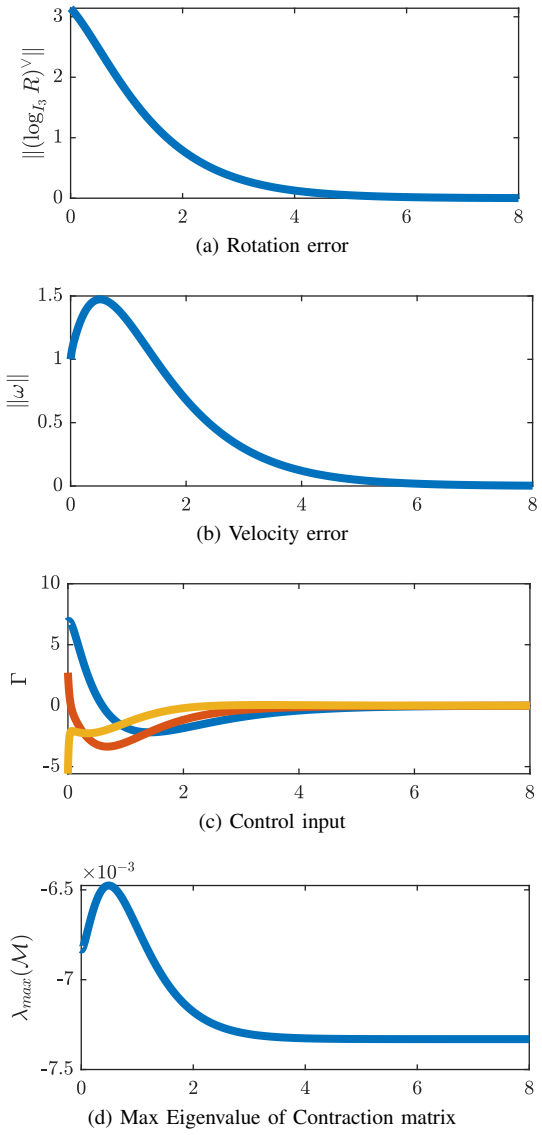

(a) Rotation error

(b) Velocity error

(c) Control input

(d) Max Eigenvalue of Contraction matrix

Fig. 1: Simulation results using parameters from Table II. The system, starting at the maximum distance, converges exponentially (contraction metric is nonpositive 1d) to the desired rotation.

The results of our algorithm are confirmed via a simulation in Matlab R2020a using 'ode45'. The tracking errors of the closed-loop system are shown in Fig. 1. From Fig. 1a and 1b, it can be concluded that the system starting at the maximum rotation away and experiencing angular speeds greater than $\|\omega\|_{max} = 1$ converges, seemingly with an exponential rate. Additionally, the control torque, Fig. 1c, is continuous and smooth which is desirable.

Exponential convergence of the system can be verified by analyzing the contraction matrix $\mathcal{M}$. The largest eigenvalue of the matrix $\mathcal{M}$ is shown in Fig. 1d. As expected, the largest eigenvalue is always nonpositive thus confirming global exponential convergence by contraction theory. Furthermore, the simulation results suggest that tighter bounds on the contraction matrix (and convergence rate) can be obtained. In particular, the general Gershgorin disc theorem produces conservative bounds on the eigenvalues. There exist a plethora of modified Gershgorin theorems that may produce tighter bounds (such as resizing of the discs via a similarity transformation); this will be explored in future work.

V. Conclusion

We have shown that a simple geometric PD controller can globally, exponentially stabilize 3-D rigid body rotations. The controller achieves this by following a reference trajectory that is designed and tuned in tandem with the controller itself. Stability of the system is proved using contraction theory combined with optimization. The result is a convex optimization problem that uses the linear matrix inequalities stemming from the contraction metric bounding the minimum convergence rate. Additionally, we proposed a way to automatically choose suitable controller gains and reference trajectory parameters that optimizes the convergence bound.

In future work, we plan to investigate other cost functions on $SO(3)$, and methods to tighten the eigenvalue bounds. Additionally, we want to apply our framework to the manifold of three-dimensional rigid poses $SE(3)$. We expect our framework to generalize well to any manifold (and product manifolds) of interest.

References

[1] R. Mahony, V. Kumar, and P. Corke, "Multirotor Aerial Vehicles: Modeling, Estimation, and Control of Quadrotor," *IEEE Robotics and Automation Magazine*, vol. 19, no. 3, pp. 20–32, 2012.

[2] M. D. Shuster, "A Survey of Attitude Representations," *Journal of the Astronautical Sciences*, vol. 41, pp. 439–517, Oct. 1993.

[3] D. E. Koditschek, "The application of total energy as a lyapunov function for mechanical control systems," *Contemporary Mathematics*, vol. 97, p. 131, 1989.

TABLE I: System and Algorithm 1 Parameters

Parameter	Value	Description
J	$\mathrm{dg}(\mathrm{stack}(5,2,1))$	Inertia matrix with values 5,2,1
k_d	100	Rotation error gain of $gainsList$
k_v	80	Velocity error gain of $gainsList$
k_{ref}	$[1,5,10,...,100]$	Reference gains of $gainsList$
$\|\omega\|_{\max}$	1	Max init. angular speed
$\theta_{R,\max}$	$\pi/4$	Max init. dist. error R to R_{ref}
$\theta_{R_{ref},\max}$	$3\pi/4$	Max init. dist. error R_{ref} to I_3

TABLE II: Algorithm 1 Results

Parameter	Value	Description
β^*	0.4022	Guaranteed minimum convergence rate
k_d^*	106.6667	Rotation error gain
k_v^*	74.6667	Angular velocity error gain
k_{ref}^*	0.9833	Reference trajectory gain

[4] F. Bullo and R. M. Murray, "Tracking for fully actuated mechanical systems: a geometric framework," *Automatica*, vol. 35, no. 1, pp. 17–34, 1999.

[5] D. S. Maithripala, J. M. Berg, and W. P. Dayawansa, "Almost-global tracking of simple mechanical systems on a general class of lie groups," *IEEE Transactions on Automatic Control*, vol. 51, no. 2, pp. 216–225, 2006.

[6] T. Lee, M. Leok, and N. H. McClamroch, "Geometric tracking control of a quadrotor uav for extreme maneuverability," *IFAC Proceedings Volumes*, vol. 44, no. 1, pp. 6337 – 6342, 2011.

[7] N. A. Chaturvedi, A. K. Sanyal, and N. H. McClamroch, "Rigid-body attitude control," *IEEE Control Systems Magazine*, vol. 31, no. 3, pp. 30–51, 2011.

[8] K. Sreenath, T. Lee, and V. Kumar, "Geometric control and differential flatness of a quadrotor UAV with a cable-suspended load," *IEEE International Conference on Decision and Control*, vol. 1243000, pp. 2269–2274, 2013.

[9] S. Berkane, A. Abdessameud, and A. Tayebi, "Hybrid global exponential stabilization on SO (3)," *Automatica*, vol. 81, pp. 279–285, 2017.

[10] T. Lee, "Global exponential attitude tracking controls on SO(3)," *IEEE Transactions on Automatic Control*, vol. 60, no. 10, pp. 2837–2842, 2015.

[11] C. G. Mayhew and A. R. Teel, "Hybrid control of rigid-body attitude with synergistic potential functions," in *IEEE American Control Conference*, 2011, pp. 287–292.

[12] ——, "Synergistic potential functions for hybrid control of rigid-body attitude," in *IEEE American Control Conference*, 2011, pp. 875–880.

[13] T. Lee, D. E. Chang, and Y. Eun, "Attitude control strategies overcoming the topological obstruction on SO(3)," in *IEEE American Control Conference*, May 2017, pp. 2225–2230.

[14] B. Vang and R. Tron, "Geometric attitude control via contraction on manifolds with automatic gain selection," *IEEE International Conference on Decision and Control*, pp. 6138–6145, 2019.

[15] S. P. Bhat and D. S. Bernstein, "A topological obstruction to continuous global stabilization of rotational motion and the unwinding phenomenon," *Systems and Control Letters*, vol. 39, no. 1, pp. 63 – 70, 2000.

[16] R. W. Brockett, "Asymptotic stability and feedback stabilization," in *Differential Geometric Control Theory*. Birkhauser, 1983, pp. 181–191.

[17] F. Bullo and A. D. Lewis, *Geometric control of mechanical systems : modeling, analysis, and design for simple mechanical control systems*, ser. Texts in applied mathematics ; 49. New York: Springer, 2005.

[18] W. Lohmiller and J. Slotine, "On contraction analysis for non-linear systems," *Automatica*, vol. 34, no. 6, 1998.

[19] J. W. Simpson-Porco and F. Bullo, "Contraction theory on Riemannian manifolds," *Systems and Control Letters*, vol. 65, no. 1, pp. 74–80, 2014.

[20] J. C. H. Lee and P. Valiant, "Optimizing star-convex functions," in *IEEE Symposium on Foundations of Computer Science*, Oct 2016, pp. 603–614.

[21] S. Boyd and L. Vandenberghe, *Convex Optimization*. Cambridge University Press, 2004.

[22] B. Vang and R. Tron, "Non-Natural Metrics on the Tangent Bundle," *arXiv e-prints*, p. arXiv:1809.06895, Sep 2018.

[23] A. Edelman, T. A. Arias, and S. T. Smith, "The Geometry of Algorithms with Orthogonality Constraints," *SIAM Journal on Matrix Analysis and Applications*, vol. 20, no. 2, pp. 303–353, 1998.

[24] R. Horn and C. Johnson, *Matrix Analysis*, ser. Matrix Analysis. Cambridge University Press, 2013.

[25] J. C. Lagarias, J. A. Reeds, M. H. Wright, and P. E. Wright, "Convergence properties of the nelder–mead simplex method in low dimensions," *SIAM Journal on Optimization*, vol. 9, no. 1, pp. 112–147, 1998.

[26] F. C. Park, "Distance Metrics on the Rigid-Body Motions with Applications to Mechanism Design," *Journal of Mechanical Design*, vol. 117, no. 1, pp. 48–54, 03 1995.

[27] R. Tron, "Distributed optimization on manifolds for consensus algorithms and camera network localization," Ph.D. dissertation, John Hopkins University, 2012.

[28] M. Grant and S. Boyd, "CVX: Matlab software for disciplined convex programming, version 2.1," http://cvxr.com/cvx, Mar. 2014.

[29] R. H. Tütüncü, K. C. Toh, and M. J. Todd, "Solving semidefinite-quadratic-linear programs using sdpt3," *MATHEMATICAL PROGRAMMING*, vol. 95, pp. 189–217, 2003.